6 DOF Magnetically suspended and propelled mirror

V.M.G. van Acht
Eindhoven University of Technology, Eindhoven, The Netherlands, V.M.G.v.Acht@tue.nl
A.A.H. Damen
Eindhoven University of Technology, Eindhoven, The Netherlands, A.A.H.Damen@tue.nl
P.P.J. v.d. Bosch
Eindhoven University of Technology, Eindhoven, The Netherlands, P.P.J.v.d.Bosch@tue.nl
J.C. Compter
Eindhoven University of Technology, Eindhoven, The Netherlands, J.C.Compter@tue.nl

ABSTRACT

An actively controlled magnetically levitated mirror with 6 degrees of freedom (DOF) is presented. This mirror is to be used in a measurement system based on laser interferometry.

A novel magnetic topology has been developed for actuating all six DOFs of the mirror. This topology almost completely decouples the different degrees of freedom. The forces and torques are independent of the rotor angle and are proportional to the applied currents. This simplifies controller design considerably.

A contactless differential capacitive position sensor system has been designed to measure the position and orientation of the mirror. This capacitive sensor system is incorporated in the magnetic actuator topology.

1 INTRODUCTION

At the Eindhoven University of Technology, Measurement and Control Group, research is done on a very accurate contactless 3D position measurement system [4] [1]. The main part of this system is a laser deflection system consisting of a small mirror which directs the beam of a laser interferometer to a moving target with a retro reflector, using a tracking control system. (See Figure 1.) The position of the object to be measured can now be calculated using the distance measurement by the laser interferometer and two angular measurements of the mirror.

The mirror of the laser deflection system can rotate around two perpendicular axes over a large range. The position error of the optical center of this mirror is specified to be smaller than 1 [μm] (suspension). The angular accuracy of the mirror is aimed

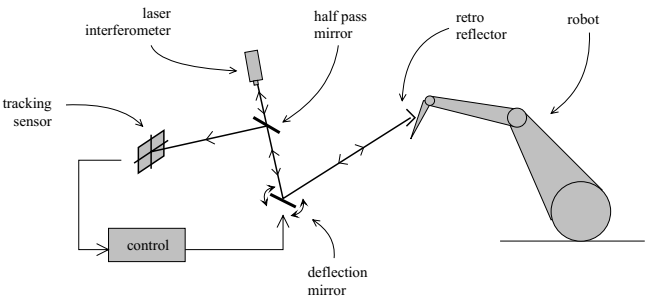

Figure 1: Complete 3D laser interferometer system.

to be smaller than < 1 [μrad] over a range of 1[rad] and with a bandwidth of > 100 [Hz] (propulsion). A rotation of the mirror around its normal axis has no optical effect, hence needs to not be controlled actively. In the presence of stick friction it is virtually impossible to satisfy these extreme accuracy requirements. Therefore magnetic bearings are currently being investigated.

As almost all practical magnetic bearings are unstable, an active position controller and a position sensor are necessary to stabilize the system. To simplify controller design, the magnetic actuator can be designed such, that the different degrees of freedom of the rotor on which the mirror is attached are almost decoupled, and that the exerted forces and torques are independent of the rotor's angles and are proportional to the applied currents. This makes that the unstable, non-linear Multiple Input Multiple Output system (MIMO) can be regarded as multiple unstable but linear Single Input Single Output systems (SISO). The position sensors have to be contactless and have sufficient range, accuracy and bandwidth to satisfy specifications. Fur-

thermore they have to be integrated in the actuator topology, which gives requirements on the sensor topology.

2 MAGNETIC TOPOLOGY

In [7] a magnetic topology for a planar active magnetic bearing (PAMB) is presented, which offers decoupling and linearity. Reluctance forces are used for the suspension of the rotor, Lorentz forces for the propulsion. Permanent magnets are used for magnet biasing, to reduce the power dissipation. However, this topology cannot be used in this application because it is optimised for large translations, whereas in this application large rotations are demanded.

2.1 Principle

A new topology has been developed [1] which is optimized for two rotations around perpendicular axes, over a large range. Another advantage of this topology is that there are no coils on the rotor. A top-view and two cross sections are depicted in Figure 2, a 3D view is shown in Figure 3. Note that the dimensions of the various magnetic elements are *not* correctly displayed in Figure 2. This picture is intended to clarify the principles of the magnetic topology. The correct dimensions are shown in Figure 3

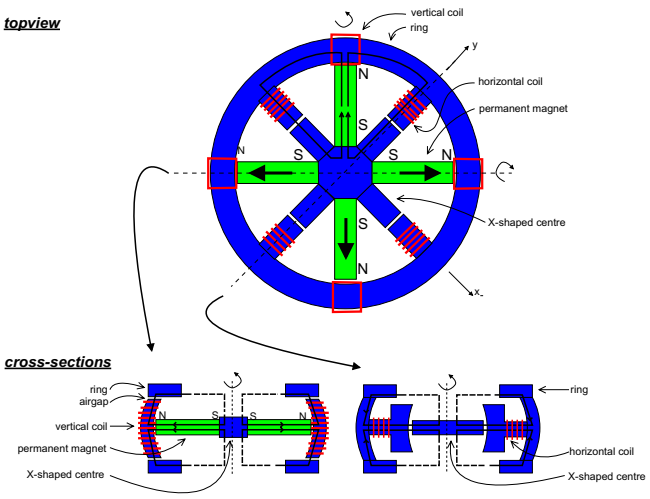

Figure 2: Magnetic topology of the actuator (2D view).

The rotor consists of four permanent magnets and a high permeability X-shaped center. The mirror is located in the center of the rotor. The stator consists of two rings with eight vertical bars in between, all constructed of a high permeability material. Around four of those bars vertical coils are wound. With these coils Lorentz forces can be generated, which can be used to exert torques around the two perpendicular rotation axes Φ and Θ of the

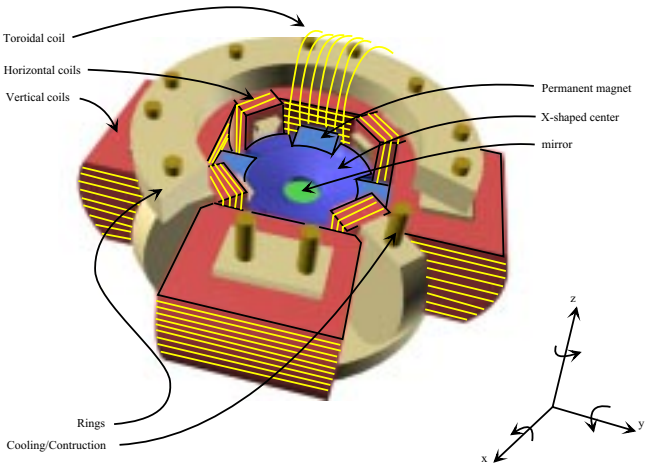

Figure 3: Magnetic topology of the actuator (3D view).

mirror, and exert forces in the z-direction. These forces and torques are proportional to the applied currents. Small airgaps exist between the vertical coils and the rings, to avoid magnetic 'short circuiting' these coils. Attached to the other four bars are four horizontal coils which can be used to exert reluctance forces in x and y direction. The relation between these reluctance forces and the applied currents is linearized because of the premagnetization by the permanent magnets. Large rotations of the rotor around the optical normal axis of the mirror Ψ are prevented by the reluctance forces between the permanent magnets and the X-shaped center of the rotor and the vertical bars on the stator. A rotation around this axis can be damped actively by the toroidal coils as depicted in Figure 3. The vertical cylinders in Figure 3 are for constructive and cooling purposes.

In contrast with the topologies in [2] and [7] the premagnetization, the reluctance forces in x and y direction and the Lorentz-forces in Φ, Θ and z direction are all independent of each other. Secondly, because of the spherical shape of the stator, the forces and torques are independent of the angle of the rotor. Thirdly, the airgap between stator and rotor is much larger than the specified position inaccuracy of the rotor, so the forces and torques are also independent of the position of the rotor, around this operating point. This makes that x, y, z, Φ and Θ are decoupled.

In [1] finite element simulation results of a 2D model of this 3D topology are presented. The 2D-model is chosen such that it incorporates most of the magnetic subsystems of the actual 3D topology. The simulation results are in accordance with the stated claims.

2.2 Dimensions

To increase the bandwidth and slew rate of the system, the ratio between forces and mass respectively torques and moment of inertia should be as high as possible. Simple scaling laws show that, for constant current density, reducing the radius of the rotor leads to an increase in the bandwidth and slew rate of the system. Obviously, the radius of the rotor cannot be decreased unlimited, because of manufacturing problems. Therefore a radius of 8[mm] is chosen, a compromise between bandwidth, slewrate and manufacturability.

The width of the permanent magnets and the width of the X-shaped center on the rotor should have a ratio of approximately 1 : 1, as for maximum force all the flux of two permanent magnets can go through one leg of the X-shape. When NdFeBo permanent magnets are used (remanent flux density ≈ 1[T]) and iron for the X-shaped center (saturation ≈ 2[T]), magnetic saturation is just avoided.

The thickness of the windings of the vertical coils must be optimized. If the coils are too thin, the generated Lorentz force is small because volume where the force is generated is too small. If the windings are too thick, the airgap in the flux path of the permanent magnets is large, leading to a low flux density, resulting in a decrease in efficiency. Using simplified lumped models and finite element modeling, it turned out that a winding thickness of 3[mm] is optimal.

The airgaps between the vertical coils and the stator rings have to be optimized. If the airgaps are too small, magnetic saturation and high inductance of the vertical coils occur. If the airgaps are too large, the airgap in the flux path of the permanent magnets is large, leading to a low flux density, resulting in a decrease of efficiency. Again using both lumped models and finite element modeling, it turned out that an airgap of 0.5[mm] is optimal.

3 CAPACITIVE SENSOR

As the magnetic actuator topology as presented in the previous section is unstable, a position control system is necessary to stabilize the three translational degrees of freedom x, y and z and the two rotational ones: Φ and Θ. This controller needs an accurate sensor for each of the degrees of freedom, with sufficient bandwidth and range. Furthermore the sensor needs to be contactless, not influenced by strong time varying magnetic fields and integrated in the magnetic topology.

Sometimes position sensors based on a magnetic principle[1] are used, but because of the limited amount of space available in this application the magnetic circuits of actuator and sensor cannot be well separated. This makes all magnetic sensors not accurate enough. Therefore a separate capacitive position sensor is used. As commercially available sensors cannot cope with the limited amount of space, the spherical behaviour of the rotor and its 5 degrees of freedom, a dedicated capacitive position sensor system has been designed.

[1] such as Eddy current sensors and LVDTs

3.1 Principle

To avoid influence of parasitic capacities a Contactless Differential Capacitive Position Sensor (CD-CPS) scheme is used [5]. This is depicted in Figure 4. The geometry of the sensor electrodes is such that the *ratio* between C_1 and C_2 changes with the position respectively orientation of the rotor. The third capacitor C_3 is to contactlessly measure the AC voltage on the interconnection point V_0 between C_1 and C_2. (Figure 4a.) The voltages V_1 and V_2 are given by $V_1 = \Delta \cdot \sin(\omega t)$ and $V_2 = -(1-\Delta) \cdot \sin(\omega t)$, where $0 < \Delta < 1$. This means that the two voltage sources have the same frequency ω, but suffer a 180° phase shift and that the ratio between their amplitudes can be changed by varying Δ. This value Δ is controlled by a controller. AC voltage sources with controllable amplitude often are called AM-modulators. The two voltages sources are assumed to be ideal, and it is assumed that the input current of the amplifier is negligible in comparison to the current flowing through C_1 and C_2 at a given frequency ω.

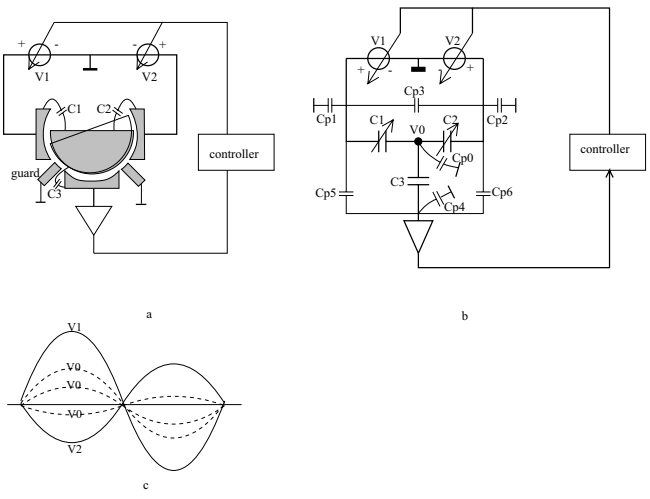

Figure 4: Contactless differential capacitive position sensor principle.

The voltage V_0 is defined by the capacitive voltage divider C_1 and C_2 and the voltages V_1 and V_2. For a certain ratio between C_1 and C_2 and for a certain $\Delta = \Delta_0$ the voltage $V_0 = 0 \, \forall t$. (See Figure 4c.) In this situtation parasitic capacities C_{p0} and C_{p4}

have no influence on the voltage V_0. As the voltage sources are assumed to be ideal, also parasitic capacities C_{p1}, C_{p2} and C_{p3} have no influence on V_0. Only C_{p5} and C_{p6} do influence the measurement, but their value can be made very small using shielding, as will be shown in the forthcoming sections. Note that C_{p0} and C_{p4} *do* influence the sensitivity of the sensor system, but not its accuracy.

The controller is designed such that Δ is regulated to this particular value Δ_0. The controller does so by contactlessly measure the voltage on node 0 via C_3 and controlling this voltage to 0 using a synchronous AM-demodulator. The necessary value $\Delta = \Delta_0$ is a measure for the ratio between C_1 and C_2 and thus for the position respectively orientation of the rotor.

In Figure 4 two guard electrodes are draw around the 'sensing'-electrode C_3. These are to minimise the value of C_{p5} and C_{p6}. When the guard electrodes are not connected to ground (as they are in Figure 4), but to the output of the amplifier, the value of C_{p4} is reduced enormously. This increases the sensitivity of the sensor considerably. This method is called *bootstrapping* [3].

3.2 Extending to more degrees of freedom

Because only a limited amount of space is available for the sensor in the laser deflection system, it is not possible to use 5 completely independent position sensors. Therefore the measurement system has been expanded to more degrees of freedom with a minimum of extra space requirements.

It is possible to use only one 'sensing'-capacitor (C_3 in Figure 4) for all degrees of freedom, when *frequency multiplexing* or *time multiplexing* are used. Also *quadrature multiplexing* could be used, if only two degrees of freedom were to be measured. All these multiplexing schemes give the diagram as in Figure 5. For every degrees of freedom two sets of voltage sources V_{1*} and V_{2*} and two sets of capacitors C_{1*} and C_{2*} are used, but only *one* capacitor C_3 from node 0 to the amplifier. This saves precious space.

When using frequency multiplexing, different modulation frequencies $\omega_x, \omega_y, ...$ are used for different degrees of freedom. All the electrodes are connected to their modulators simultaneously. For each extra modulation frequency also an extra demodulator and control system are necessary.

When time multiplexing is used, the signals of $x, y, ...$ are not modulated on different frequencies, but in different time slots. While the electrodes belonging to a certain degree of freedom are connected to the modulators, the other electrodes are connected to ground. Only one demodulator is necessary, however the output of this demodulator must

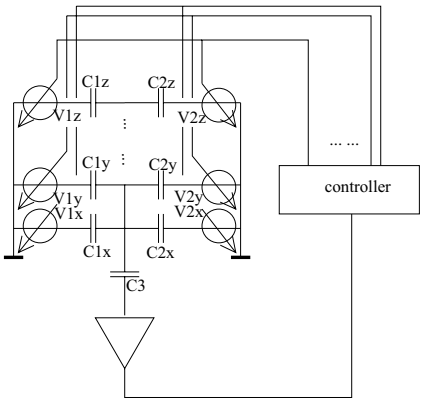

Figure 5: Principle of multi DOF contactless differential capacitive position sensor.

be passed through individual sample and hold circuits for the different degrees of freedom.

In both cases, the electrodes for other degrees of freedom than the one under consideration can be regarded as parasitic capacities to ground [2]. And as already shown in the previous section, parasitic capacities from node 0 to ground do not influence the accuracy of the sensor system. This means that the different degrees of freedom do not influence each other.

Not only the same 'sensing'-electrode can be used for all degrees of freedom, also the 'sourcing'-electrodes can be shared by different degrees of freedom using time- or frequency multiplexing, as will be shown in section 3.4.

3.3 Simplifying electronics

In the description of the measurement principle in the previous sections, sinusoidal signals were assumed for V_1 and V_2. However, as the measurement principle is independent of the frequency ω and superposition holds, any waveform can be used. Hence square waves are used, which can be generated much simpler.

In Figure 6 the electronics for the differential modulators are shown. As can be seen, it consists of only two very accurate DC reference voltage sources and two switches. V_i represents the output of the controller. Each switch can be build by two MOSFETs. In Figure 6c the output waveforms V_{o1} and V_{o2} are shown. As only the AC signal of node 0 is measured by the sensing capacitor C_3, the DC levels of V_{o1} and V_{o2} have no influence.

In Figure 7 the electronics for the multiplier in the demodulator are shown. It consists only of a buffer,

[2] All the 'sourcing' capacitors are connected to a voltage source. Voltage sources with a frequency other than the frequency under consideration can be regarded as short circuits.

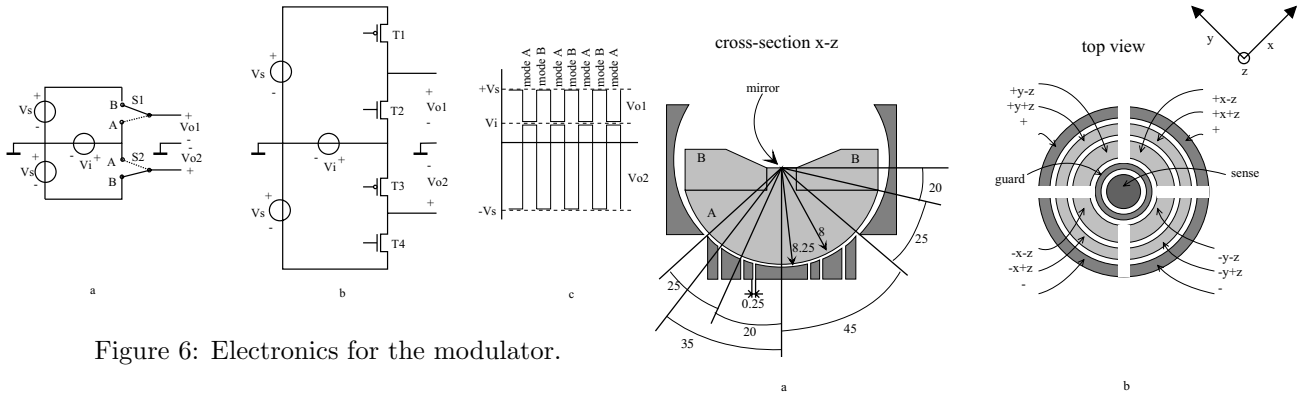

Figure 6: Electronics for the modulator.

an inverter and one switch. In Figure 7b the input and output signals of the multiplier are shown. The multiplier should be followed by a normal low pass filter to eliminate demodulation products around the frequency 2ω

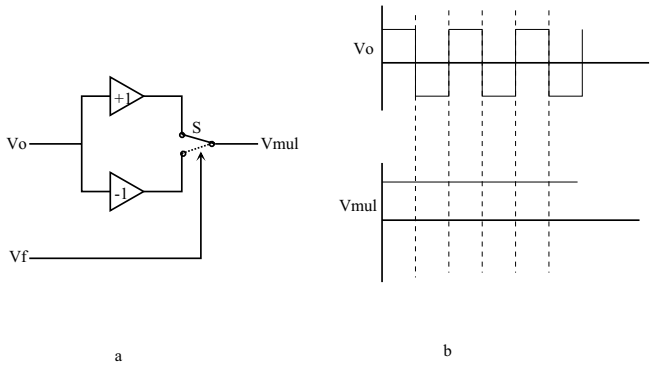

Figure 7: Electronics for the demodulator.

It is possible to use a kind of 'sample and hold' circuit after the multiplier, to eliminate the 'noise' in the output signal at the switching moments. This improves the signal to noise ration of the sendor considerably.

In section 3.4 modulation signals for different degrees of freedom must be 'added' on one electrode. This can be simply done by adding some more switches in the modulator and alternate switching between $V_{i,x}$ and $V_{i,y}$, when using time multiplexing.

3.4 Sensor Topology

In Figure 8a a cross section of the electrode topology of the 5DOF contactless differential capacitive position sensor is shown. In Figure 8b the topview is depicted. Elements A and B form the rotor, where A is a spherical shaped conductor and B are parts of the magnetic actuator. The mirror is manufactured on the top of part A, so that the mirror surface is perfectly aligned with the center of the spherical shape of A.

Figure 8: Electrode topology of 5DOF capacitive position sensor.

The guard electrode surrounds the sensing electrode in the center of the topology. If the width of the guard is chosen to be a few times the airgap between stator and rotor, C_{p5} and C_{p6} are negligible to C_1, C_2 and C_3. The guard should be connected to the output of the amplifier.

Because the top side of the rotor has to be free for the optics, the electrodes for x and y on the bottom are also used to measure z. This is done by splitting these electrodes in two (giving all eight combinations of $\pm x \pm z$ and $\pm y \pm z$) and using time multiplexing. Because the $\pm x + z$ and $\pm y + z$ electrodes have an other angle to the horizontal plane than the $\pm x - z$ and $\pm y - z$ electrodes, a variation in height of the rotor changes the ratio $\frac{(\pm x+z)+(\pm y+z)}{(\pm x-z)+(\pm y-z)}$. Hence the CDCPS principle can be used. Note that the sensitivity for z is less than for x and y.

Figure 8a shows that the electrodes for Φ and Θ are located in the space of the magnetic actuator. However, this is not a problem, as a thin conductive layer can be manufactured on parts of the magnetic topology of the stator [3], which can be used as the electrodes for Φ and Θ. These thin conductive layers do not influence operation of the magnetic actuator.

Tolerances on the assembly of the sensor electrodes can be relaxed, as all non-linearity and coupling in the 5DOF position sensor can be calibrated for. This simplifies manufacturing considerably, but introduces a (tedious) step of calibration.

4 CONCLUSIONS

In this paper a magnetic topology has been presented for a magnetically suspended and propulsed mirror to be applied in a 3D laser interferometer. The topology is optimized for rotations around two perpendicular axes over a large range, and offers de-

[3] Namely on the poleshoes of the four horizontal coils

coupling and linearity. This simplifies controller design for the unstable system considerably.

A contactless capacitive position sensor, able to measure all degrees of freedom with satisfactory accuracy and bandwidth is presented. The topology of the electrodes of the sensor is such that it can be incorporated in the magnetic actuator topology.

5 FUTURE WORK

A test set-up for the contactless differential capacitive position sensor with one degree of freedom has been built and tested with success [6]. The accuracy of this proto-type sensor was $1 : 10^4$. Currently, the 5DOF sensor and the magnetic topology as presented in sections 2 and 3 are being manufactured. In the near future the sensor will be tested and roughly calibrated. Using the calibrated sensor system also the magnetic actuator can be calibrated by measuring induced voltages on the coils by a random movement of the rotor and using reciprocity, correlation techniques and black box modeling.

Once a model with satisfactory accuracy of both sensor and actuator is available, a controller can be designed which stabilizes the magnetic suspension and propulsion in all 5 degrees of freedom. As the magnetic topology is such that actuators are linear and decoupled, simple decoupled PID controllers will probably work.

To avoid problems during lift-off of the unstable system, a special coating is applied on the stator and the rotor (in the airgap between stator and rotor), assuring that the rotor is approximately in the center of the stator. This reduces the cogging force and prevents that the system is far from its (linearised) operating point.

The controller will be implemented on a digital computer, and tested on the physical plant. The coating between stator and rotor prevents damage to the magnetic actuator or the sensor electrodes if the controller is unable to stabilize the system the first time.

Once a stabilizing controller has been found, optical measurement techniques can be used to calibrate the sensor to great accuracy and closed loop identification can be applied to find a more accurate model of the actuators. If necessary, a better controller can be designed.

ACKNOWLEDGEMENT

We would like to thank prof. E.M.H. Kamerbeek for his contributions to the magnetic topology and dr. A. Veltman and H.P.M. Goossens for their contributions to the contactless differential capacitive position sensor.

References

[1] Acht van V.M.G., A.A.H. Damen, P.P.J. v.d. Bosch and E.M.H. kamerbeek
Topology of six degrees of freedom magnetic bearing
Journal of Applied Physics, May 1, 2000, Volume 87, Issue 9, p. 6920-6922

[2] Auer F.
A combined electromagnetic suspension and propulsion for positioning with sub-micrometer accuracy
PhD thesis, 1995, Delft University of Technology, The Netherlands, Delft University Press

[3] L.K. Baxter
Capacitive sensors, Design and applications
IEEE Press Series on Electronics Technology, Piscataway, USA, ISBN 0-7803-1130-2

[4] P.P.J. van den Bosch and A.A.H. Damen
Air and magnetic bearings for a laser beam deflection unit
Proc. ACC '97, Albuquerque, USA, June 1997, p. 2987-2991

[5] A. H. Falkner
The use of capacitance in the measurement of angular and linear displacement
IEEE Transactions on instrumentation and measurement, Vol. 43, No. 6, p. 939-942

[6] H.P.M. Goossens
Differentieel capacitief positie sensor systeem...
Stageverslag, 1999
Eindhoven University of Technology, The Netherlands, Department of Electrical Engineering
(In Dutch)

[7] A. Molenaar, E.H. Zaaier, H.F. van Beek
A novell low dissipation long stroke planar magnetic suspension and propulsion stage
proc. ISMB-6, Cambridge, USA, August 1998, p. 650-660